Changes in membrane organization upon spontaneous insertion of 2-hydroxylated unsaturated fatty acids in the lipid bilayer

Alena Khmelinskaia[†‡], Maitane Ibarguren[‖‡], Rodrigo F. M. de Almeida[†*], David J. López[‖*], Vanda A. Paixão[†], Hasna Ahyayauch[§¶], Félix M. Goñi[§] and Pablo Escribá[‖]

[†]Centro de Quimica e Bioquimica, DQB, Faculdade de Ciências da Universidade de Lisboa, Campo Grande, Ed. C8, 1749-016 Lisboa, Portugal

[‖]Laboratory of Molecular Cell Biomedicine, University of the Balearic Islands-Lipopharma Therapeutics, S. L., Palma, Spain

[§]Unidad de Biofísica (Centro Mixto CSIC-UPV/EHU), Departamento de Bioquímica, Universidad del País Vasco, Bilbao, Spain.

[¶]Institut de Formation aux Carrières de Santé de Rabat, Avenue Hassan II, Kilomètre 4,5 Rabat, 10000 Marocco

Keywords: free fatty acid, lipid membrane structure, hydroxylated fatty acid, lipid phases, membrane microdomains, gel, liquid ordered, liquid disordered, fluorescence spectroscopy, ITC, membrane model systems, membrane order.

ABSTRACT

Recent research regarding 2-hydroxylated fatty acids (2OHFA) showed clear evidence of their benefits in the treatment of cancer, inflammation and neurodegenerative disorders such as Alzheimer´s disease. Monolayer compressibility isotherms and isothermal titration calorimetry of 2OHFA (C18-C22) in phosphatidylcholine: phosphatidylethanolamine: sphingomyelin: cholesterol (1:1:1:1; mol ratio), a mixture that mimics the composition of mammalian plasma membrane, were performed to assess the membrane binding capacity of 2OHFA and their natural, non-hydroxylated counterparts. The results show that 2OHFA are surface-active substances that bind membranes through exothermic, spontaneous processes. The main effects of 2OHFA are a decrease in lipid order, with a loser packing of the acyl chains, and decreased dipole potential, regardless of the 2OHFA relative affinity for the lipid bilayer. The strongest effects are usually observed for 2-hydroxyarachidonic (C20:4) acid and the weakest one for 2-hydroxydocosahexaenoic acid (C22:6). In addition, 2OHFA cause increased hydration, except in gel phase membranes, which can be explained by the 2OHFA preference for membrane defects. Concerning membrane dipole potential, the magnitude of the reduction induced by 2OHFA was particularly marked in liquid-ordered (*lo)* phase (cholesterol/sphingomyelin rich) membranes, those where order reduction was the smallest, suggesting a disruption of cholesterol-sphingolipid interactions that are responsible for the large dipole potential in those membranes. Moreover 2OHFA effects on glioma cell model membranes (liquid disordered, *ld*/*lo* coexistence) was larger than for both *lo* and *ld* phases separately, suggesting a role for *ld*/*lo* coexistence, possibly due to domain size and interfacial lipid. The specific and marked changes induced by 2OHFA in several membrane properties suggest that the initial interaction with the membrane and subsequent reorganization might constitute an important step of their mechanisms of action.

INTRODUCTION

The composition of the cell membrane in terms of fatty acids (FA), mostly found as part of phospholipids and sphingolipids, can modulate important signaling transduction pathways, and ultimately control vital physiological processes. For instance, high olive oil consumption, which is enriched in oleic acid (OA), reduces the incidence of cardiovascular diseases and cancer [1, 2]. Docosahexaenoic acid (DHA) and eicosapentaenoid acid (EPA) have also been associated with the prevention of cardiovascular diseases and cancer [3], as well as with a strong neuroprotective effect by reducing amyloid β42 production [4]. In this sense, during the last few years, a number of 2-hydroxylated fatty acids (2OHFA) (Fig. 1) have been designed as active drugs for lipid therapy related to cardiovascular issues [5], cancer [6, 7], inflammation [8], obesity[9] or Alzheimer´s disease [10]. 2-hydroxyoleic acid (2OHOA), the most studied molecule of the group, may exert its anti-tumor effects through different mechanisms, including the induction of apoptosis or cellular differentiation and autophagy, where the sphingomyelin cell content seems to be involved [6, 7]. 2-hydroxyarachinodic acid (2OHARA) has a highly anti-inflammatory effect through interference with cicloxygenase expression and enzymatic activity [8] and 2-hydroxydocosahexanoic acid (2OHDHA) delivered promising effects in Alzheimer's disease [10].

Free fatty acids (FFAs) are minor components of biological membranes counting for *ca.* 1-2% of total lipids [11]; however, they are important components in certain membranes such as in the small intestine brush border where their levels can reach *ca.* 20% of total lipids [12]. Moreover, FFAs affect basic processes common to various cell types which may answer the question about how these simple molecules can be involved in different seemingly unrelated pathologies. The mechanism of action of FAs, and 2OHFAs, on cell signaling has been proposed to be linked to changes in membrane structure and function [13]. At high concentrations, the incorporation of FFAs into the lipid bilayer has a general solubilizing effect due to their ability to form micelles [14]. However, at smaller and possibly more physiologically relevant concentrations, FFA may exert more subtle effects slightly changing important biophysical parameters which have been shown to modulate the activity of membrane proteins [15, 16, 17], such as lateral pressure [18], membrane fluidity [19] or microdomain reorganization [13]. These membrane biophysical properties can change

due to either incorporation of FFAs, or due to alterations in FA composition of acylated lipids. Nevertheless, the mechanism of action of these molecules is not fully understood.

The majority of studies concerning FAs and 2OHFAs examine the effect of the unsaturation/chain length/hydroxylation on lipid membranes through the use of phospholipids with different acyl chain composition in model membranes, or through metabolically induced changes in acyl chain compositions of cell membranes [20, 21, 22]. An increase in the number of double bonds in the *sn*-2 chain of monounsaturated phosphatidylcholine (PC) results in an increase in the lateral diffusion in one-component PC bilayers [23]. In the same study a phase separation into liquid-disordered (l_d) and liquid-ordered (l_o) phases was observed in a ternary system of PC/egg sphingomyelin (SM)/cholesterol (Chol) for more unsaturated PCs, due to the increasing difficulty of incorporation of more unsaturated lipid into the highly ordered SM/Chol matrix. The ability of polyunsaturated fatty acids (PUFAs) to modify membrane lipid raft structure and composition, contributes to membrane protein function modulation and activation of signaling cascades such as triggering the pro-apoptotic ceramide linked pathway [24, 25]. In this context, treatment with 2OHOA leads to a marked increase in SM levels in cancer cells (in which basal SM levels are markedly low) among other lipid metabolism alterations which strongly influenced membrane biophysical properties [7].

Nevertheless, the effect of direct addition of FAs, or increased concentration of free FAs, e.g. due to activation of PLA_2 [17, 26, 27], can be different from FA incorporation into phospholipids. The effect of the direct insertion of FFA in bilayer elastic properties has been described, and it was concluded that there were noticeable consequences of PUFAs addition, such as DHA, whereas saturated and monounsaturated FFA were relatively inert [16]. The effects can be partially explained by negative curvature induction and plasma membrane lipid raft structure changes [14]. Also, the impact of different OHFAs on dimyristoylphophatidylcholine (DMPC) model membranes phase transition was assessed through DSC studies as a function of chain length and position of the attached hydroxyl group, showing a tendency to reduce the lipid order as deduced by the reduction of the solid-to-liquid crystalline phase transition temperature (T_m) values by FAs with unsaturations and hydroxyl groups in the hydrophobic core of the membrane [28]. The presence of

free 2OHOA in lipid bilayers was hypothesized to contribute for membrane increased hydration and fluid domain organization [29], having a general fluidifying effect in lipid membranes [13, 30, 31]. Nonetheless, 2OHOA, 2OHARA and 2OHDHA were shown to induce a higher hydration level and increased disorganization, through increased acyl chain mobility and decreased l_o domain size and proportion when added to membrane model systems [13]. Thus, it is important to know the effect of this addition and understand its contribution in comparison to 2OHFA incorporation into phospholipids, and even sphingolipids [32, 33, 34]. This knowledge will allow a better understanding of the molecular mechanism of 2-hydroxylated fatty acids on their therapeutic action.

The present study examines the interactions of synthetic, unsaturated 2-hydroxylated fatty acid molecules with potentially unique therapeutic properties, and their natural occurring counterparts with model membranes mimicking different lipid phases and phase coexistence situations, in order to obtain a deeper understanding of their molecular mechanisms of action. Here, it is shown that the ability of 2OHFAs to reorganize the lipid bilayer microdomains towards a less organized state is not directly related to the degree of interaction of FAs and 2OHFAs with the membrane. The strongest changes are induced by 2OHARA suggesting an important role for the initial interaction with the membrane and the domain reorganization in its mechanism of action. In single phase bilayers, small changes in membrane order/compactness are observed, which are enhanced when l_d / l_o phases coexist. Moreover, marked changes occur in hydration properties, particularly in l_o bilayers, pointing overall to a role in membrane microdomain organization in the initial interaction of the 2OHFA with the target cells.

MATERIALS AND METHODS

Materials— 1-palmitoyl-2-oleyl-sn-glycero-3-phosphatidylcholine (POPC), liver bovine phosphatidylethanolamine (PE), 1-palmitoyl-2-oleyl-sn-glyero-3-phosphatidylethanolamine (POPE), egg chicken SM, *N*-palmitoyl-SM (PSM) and Chol were from Avanti Polar Lipids (Alabaster, AL). DMSO, OA and arachidonic acid (ARA) were purchased to Sigma-Aldrich (St. Louis, MO). EPA and DHA were obtained from BASF Pharma (Callanish, UK). 2OHOA, 2OHARA and 2OHDHA were kindly provided by Lipopharma Therapeutics S.L. (Palma, Spain). Chloroform and methanol were bought to Scharlab (Barcelona, Spain) or to Fluka (St. Louis, MO,

USA). Ethanol was also purchased to Fluka. Nuclepore and Anotop filters were purchased to Whatman (Kent, United Kingdom). The probe *trans*-parinaric acid (*t*-PnA) was obtained from Santa Cruz Biotechnology (Dallas, TX, USA); 1,6-diphenol-1,3,5-hexatriene (DPH) and di-4-ANEPPS were purchased to Invitrogen, Molecular Probes (Barcelona, Spain).

Preparation of lipid vesicles— For isothermal titration calorimetry experiments, large unilamellar vesicles (LUV) composed of POPC:PE:SM:Chol (1:1:1:1; mol ratio) were generated in 10 mM Hepes, 1 mM EDTA, 100 mM NaCl, pH 7.4 using 200 nm filters according to previously described methods [35]. Quantitative analysis of the lipid composition of LUVs was performed by thin layer chromatography in order to confirm that the final composition did not differ significantly from the initial lipid mixture.

For fluorescence measurements, appropriate volume of POPC, POPE, PSM and Chol stock solutions were mixed to mimic the lipid composition of mammalian plasma membrane (equimolar mixture), U-118 glioma cell membrane [7] and the main types of lipid phases (gel, l_o and l_d) [36] (Table 1). Lipids were suspended in 10 mM Hepes, 150 mM NaCl, 0.1 mM EDTA, pH 7.4 to obtain multilamelar vesicles (MLV) suspensions at a final lipid concentration of 2 or 3 mM. To obtain LUV, MLV suspensions were extruded using an Avanti Mini-Extruder and Nuclepore polycarbonate filters (100 nm pore diameter). Aliquots from the total LUV suspension with a final lipid concentration of 0.5 mM (which ensures efficient incorporation of 2OHOA into the lipid bilayer [30]) were labeled with either DPH or *t*-PnA or di-4-ANEPPS (1/500 probe/lipid ratio) added from stock ethanol solutions and incubated for 1h at 50 ºC [37, 38] . For a direct comparison with the ITC results, the experiments with the equimolar mixtures were also performed for 0.1 mM lipid, to preserve the same lipid/fatty acid proportions, and using the same hydration buffer as in the ITC experiments yielding essentially the same results (not shown). Ethanol was added in a concentration that did not disturb lipid bilayer properties [39]. The suspension was slowly brought to room temperature and allowed to equilibrate, then 20 mol% 2OHFA was added and incubated at least 1 h before fluorescence measurement.

Surface pressure measurement— Changes in surface pressure (Π) were measured in a Delta Pi-4 Kibron instrument (Helsinki, Finland) equipped with 4-channel Langmuir tensiometers.

Natural and synthetic fatty acids were dissolved in DMSO at a final concentration of 1 mM and they were injected into the subphase of a through filled with 10 mM Hepes, 1 mM EDTA, 100 mM NaCl, pH 7.4, under continuous stirring. After addition of the FA and 2OHFA, the system was left to equilibrate for at least 10 min and the Π value was recorded. Analysis of FA or 2OHFA insertion into lipid membranes were performed using POPC:SM:PE:Ch (1:1:1:1; mol ratio) as a membrane substrate. In brief, the lipid mixture dissolved in chloroform:methanol (2:1; vol:vol) was added drop-wise on the buffer surface to reach the initial surface pressure (Π_i). Since the Π_i value cannot be controlled accurately enough, values of 0.3 – 0.5 mN/m over or above the desired values were considered acceptable. The organic solvent was left to evaporate and the FA or 2OHFA dissolved in DMSO was injected into the subphase until the Π value did not change longer. Increases in Π were plotted against the Π_i values and data were fitted to a straight line as described elsewhere[40]. The small changes in Π_i induced by DMSO alone were subtracted from the raw data.

Isothermal Titration Calorimetry— ITC measurements were performed at 298 K in a VP-ITC microcalorimeter (MicroCal, Inc.,Northampton, MA). 2 μl of a 10 mM LUV suspension were injected into an ITC cell containing 30 μM FA or 2OHFA. The thermodynamic parameters of 30 injections were recorded and analyzed using the MicroCal Origin software. The apparent binding constant Ka (Kd =1/Ka), and enthalpy ΔH° were obtained from the fitting curve analysis of isotherms. The model for the calculation of Kd shown in the present study has been extensively used elsewhere[41, 42], and although it represents a global measurement of the free energy of interaction, which could in principle be decomposed in several partial steps/contributions, it allows the study of similarities and differences between the studied natural and synthetic fatty acids. Gibbs free energy (ΔG°) and entropy (ΔS°) of binding are determined from the expression

$$\Delta G° = \Delta H° - T\Delta S° = -RT\ lnKa \qquad \textit{(Equation 1)}$$

Fluorescence measurements and data analysis— Fluorescence measurements were done at 24 ºC using a Horiba Jobin Yvon Spex Fluorolog 3-22/Tau 3 spectrofluorometer (Kyoto, Japan).

For steady-state fluorescence anisotropy measurements, the samples were excited at 303 nm, 358 nm and 465 nm and emission collected at 404 nm, 430 nm and 610 nm, for *t*-PNA, DPH and di-4-ANEPPS labeling respectively. For wavelength scans, the excitation and emission wavelengths are indicated in the results section. The membrane dipole potential was measured through the excitation ratio of intensities at 420 nm / 520 nm of di-4-ANEPPS with emission at 610 nm [37, 43]. The steady-state anisotropy (<*r*>) was calculated according to the Eq. 2 [44],

$$< r >= \frac{(I_{VV} - \frac{I_{HV}}{I_{HH}} \times I_{VH})}{(I_{VV} + 2\frac{I_{HV}}{I_{HH}} \times I_{VH})} \qquad \textit{(Equation 2)}$$

in which I_{XY} represent the emission intensity reading with vertical (*V*) or horizontal (*H*) orientations of the excitation (*X*) and emission (*Y*) polarizers. An adequate blank was subtracted from each intensity reading and each set of four intensity components for each sample was measured seven times. 3 nm slits were used for DPH and 4 nm slits for *t*-PNA and di-4-ANEPPS.

For time-resolved measurements by the single photon counting technique (SPT) nanoLED N-310, N-370 and N-460 were used for the excitation of *t*-PNA, DPH and di-4-ANEPPS, and emission wavelength were 404 nm, 430 nm and 610 nm, respectively. The resolution of the detection system was 50 ps. The number of counts on the peak channel was 10,000-20,000 for each sample. The time scale used for the analysis varied between 0.05552 ns/channel (DPH, di-4-ANEPPS, and *t*-PnA in l_d membranes), 0.11104 ns/channels (*t*-PnA in l_d / l_o and l_o membranes), 0.22312 ns/channel *t*-PnA in gel membranes. The bandwidth was adjusted from the maximum value allowed by the instrumental setup (15 nm) to ensure an SPT regime (15nm for di-4-ANEPPS; 6 – 15 nm for both *t*-PnA and DPH). Data analysis was performed through a non-linear minimum square iterative re-convolution method based on the Marquardt algorithm, using the Time-Resolved Fluorescence Anisotropy Data Processor 1.4 program to obtain the fitting parameters, as previously described [32].

For a fluorescence intensity decay described by a sum of exponentials, i.e.,

$$i(t) = \sum_i a_i \exp\left(\frac{-t}{\tau_i}\right) \qquad \textit{(Equation 3)}$$

α_i and τ_i are the normalized amplitude and lifetime of component i, respectively. The intensity-weighted mean fluorescence lifetime is given by

$$< \tau >= \frac{\sum_i a_i \tau_i^2}{\sum_i a_i \tau_i} \qquad \textit{(Equation 4)}$$

Two to four exponentials were required to describe each of the fluorescence intensity decays, depending on the lipid mixture composition and the probe in analysis. The background (obtained with the correspondent blank sample) was subtracted from the decay.

All the data are expressed as the mean ± standard deviation of at least three independent samples.

Fatty acid oxidation assay— Fatty acid oxidation was measured by light absorption at 245 nm[45]. 1 mg/ml OA or 2OHOA and 0.05 mg/ml ARA, 2OHARA, DHA or 2OHDHA were incubated at room temperature in 2 ml of 10 mM Hepes, 1 mM EDTA, 100 mM NaCl, pH 7. The incubation time was 60 minutes, which exceeds the experimental conditions of the surface pressure measurements. Fatty acids were extracted by addition of chloroform:methanol (2:1, by vol), following evaporation of the lower organic phase. The lipid film was resuspended in ethanol and absorption at 245 nm was recorded in a Varian Cary 300 Bio spectrophotometer (Palo Alto, CA). For negative oxidation controls, lipids were incubated in the presence of 50 μM butylated hydroxytoluene and they were immediately extracted as above. As a control for oxidative state, FA or 2OHFA solutions were incubated at room temperature for 24 h in the absence of EDTA and in the presence of 12 μM $CuSO_4$.

RESULTS AND DISCUSSION

Incorporation of fatty acids in model membranes— Fatty acids are amphiphilic molecules with a propensity to insert in lipid bilayers. Previous studies have shown, by means of Molecular Dynamics models, that incubation of both OA and 2OHOA with phosphatidylcholine bilayers provokes aggregation of FAs in the first steps of the simulations, followed by their spontaneous insertion into the bilayer [31]. In order to check the tensioactive properties and the tendency of natural and synthetic FAs to interact with lipid membrane, surface pressure studies were performed at the air-water interface. Fig. 2 A-C shows mean curves of equilibrium values of Π after addition of different FA or 2OHFA concentrations into the subphase of a tensiometer

through. 2OHFA and FA caused a dose-dependent increase in Π with a maximum value of ca. 40 mN/m when using 30 μM OA or 2OHOA (Fig. 2A). However, when polyunsaturated ARA, 2OHARA, DHA and 2OHDHA (Fig. 2B-C) molecules were used, the plateau ~35-40 mN/m was reached at higher fatty acid concentration (ca. 50 μM). This concentration value probably represents the point at which FA and 2OHFA micelles start being formed, so that a regime of monomers-in-solution in equilibrium with monomers-at-the interface is being replaced by a more complex equilibrium between monomers (interface), monomers (solution) and micelles (solution). These results show that these FA and 2OHFA molecules are surface-active lipids with a critical micellar concentration in the 30–50 μM range, a concentration used for the study of incorporation of 2OHFA or FA into preformed phospholipid model membranes. Critical micellar concentration values are notoriously dependent on the method used. In this work, we have used the surface pressure method, that is widely accepted, and has the advantage of not using external probes[46, 47, 48].

The insertion of 2OHFA and FA into phospholipid monolayers was tested using the Langmuir balance, with preformed POPC:PE:SM:Chol (1:1:1:1; mol ratio) monolayers at the air–buffer interface, and each of the FA or 2OHFA injected into the subphase. Increases in lateral pressure due to FA or 2OHFA insertion depended strongly on the Π_i value. The increments of surface pressure ($\Delta\Pi$) upon 2OHFA or FA insertion into the preformed phospholipid monolayer were plotted as a function of Π_i (Fig. 2 D-F). A straight line was fitted to the data , and extrapolation to $\Delta\Pi=0$ yielded the maximum monolayer surface pressure after the insertion of the studied molecule into the monolayer. 2OHFA or FA may become inserted into monolayers resembling cell membrane composition up to *ca.* 40-46 mN/m for either the polyunsaturated FA or 2OHFAs. This is important because cell membranes are considered to support a lateral pressure ~30 mN/m [49] albeit with large fluctuations around this average value. Thus, the data in Fig. 2 D-F indicate that these molecules can insert easily into cell membranes, in agreement with their well-known effects at the cellular level [7]. No noticeable differences were registered between 2OHFA and their natural non-hydroxylated FA analogues. Moreover, the maximum pressure supported by

POPC:PE:SM:Cho (1:1:1:1, mol ratio) monolayers is ~44-46 mN/m (data not shown). According to Fig.2 D, E and F, the collapse pressure of the monolayer upon insertion of FA or 2OHFA reaches a similar Π value, indicating that neither FA nor 2OHFA affect the monolayer stability to collapse.

Lipid oxidation was determined spectrophotometrically in order to discard any influence of FA and 2OHFA degradation during the course of the experiment (Fig. S1, in Supplementary Material). Neither FA nor 2OHFA were oxidized in the conditions of the experiments, as described in Material and Methods. Concerning the effect of DMSO solvent on lipid membranes, it has already been described that under our conditions DMSO does not alter the structure of giant unilamellar vesicles (GUVs) or LUVs [13]. In addition, the small contribution of DMSO to the increase of Π was subtracted individually to each data point. Thus, the addition of 80 μl DMSO, which corresponds to the maximum volume used in the study of surface-active properties induced an increase of 1.8 mN/m, while the same volume of vehicle containing 70 μM FA or 2OHFA, yielded a Π value increment of 35-40 mN/m.

Membrane binding thermodynamic parameters of fatty acids— ITC was used to study the capacity of different natural and synthetic FA to bind to model membranes mimicking the plasma membrane composition (POPC:PE:SM:Chol; 1:1:1:1; mol ratio). Although the interaction of the FA and 2OHFA with the lipid bilayers is much more complex than the binding of a drug to a specific site in a protein, a simple model considering one binding constant gave an excellent description of the ITC data, and, as described in Materials and Methods, was used to compare the relative affinity of the molecules to the membrane and to access the total free energy of membrane fatty acid interaction, which should not be regarded just as the free energy of binding. The use of a simple model is also justified by the observation that the membrane /water partition constant of several FA, including OA and DHA, is independent or very weakly dependent on membrane composition, and is independent on FA concentration at least in the range of micromolar to tenths of micromolar [16, 50]. Table 2 shows similar relative affinity of DHA and OA to the lipid bilayers

as previous works[16], even though it was obtained from a different method, further supporting the use of the model here described.

In this context, OA (3.65 ± 0.18 μM) and 2OHDHA (4.37 ± 2.86 μM) showed a higher binding affinity to the lipid bilayer than other FA or 2OHFA molecules (Table 2). On the other hand, ARA showed the lowest affinity value (49.38 ± 11.5 μM) for the studied membrane model, while 2OHOA had an intermediate affinity (Kd = 28.92 ± 3.02 μM) (Fig. 3, Table 2). Moreover, all the binding processes were exothermic ($\Delta H^o<0$), increased the disorder of the system ($\Delta S^o>0$) and were therefore, spontaneous ($\Delta G^o<0$). No marked differences in ΔG^o values were observed for the six natural and synthetic FA studied. The spontaneity of the process is in agreement with Langmuir balance results, where it was described that all the studied natural and synthetic fatty acid molecules had a tendency to insert into the lipid membrane.

Membrane reorganization by 2-hydroxylated fatty acids – In order to study the effect of 2OHFAs in membrane organization, vesicles mimicking the lipid composition of the mammalian plasma membrane (POPC:POPE:SM:Chol, 1:1:1:1; mol ratio) were analyzed in the presence or absence or each 2OHFA by fluorescence spectroscopy (fluorescence anisotropy, lifetime and excitation/emission spectra). Three different probes, particularly sensitive to certain types of phases and/or membrane biophysical properties were used. More specifically, the global membrane order was assessed measuring DPH fluorescence anisotropy, since this probe has no preference for lipid domains and is aligned with the phospholipid acyl chain palisade [51] (and references therein). *t*-PnA is especially useful to detect the presence of a gel phase as its fluorescence lifetime is highly dependent on acyl chain packing, presenting a long lifetime component in ordered domains [32, 52]. On the other hand, di-4-ANEPPS is very sensitive to water penetration and H-bonding patterns because of the very large change of its dipole moment upon excitation in the direction of the membrane normal [53]. Due to its shallow location in the lipid bilayer as compared with the other two probes, it detects the alterations of biophysical properties mainly at the lipid headgroup / water interface region [43]. It can also be used to measure membrane

dipole potential alterations. Moreover, these properties are strongly affected by 'raft-forming' sterols [54] and thus, this probe is sensitive to Chol-enriched domains [37].

The general effect of 2OHARA and 2OHDHA in model membranes mimicking the composition of mammalian plasma membrane (POPC:POPE:SM:Chol, 1:1:1:1; mol ratio) is the reduction of lipid order and packing in the membrane (Fig. 4), as had already been shown for 2OHOA [13, 30]. This effect is manifested by a decrease of both DPH steady state fluorescence anisotropy and *t*-PnA mean fluorescence lifetime. Furthermore, this effect seems to be independent of the capacity of 2OHFA to bind to the lipid bilayer. For instance, 2OHDHA, the fatty acid derivative that binds to the assayed membranes with the highest affinity (Table 2), induces less disorganization in liposomes compared to other 2OHFAs, according to recent NBD self-quenching data [13], and mean fluorescence lifetime of *t*-PnA (Fig. 4B).

LUVs with lipid compositions corresponding to three different lipid phases at room temperature (gel, l_d and l_o) were also analyzed in order to study separately the effect of 2OHFA in bilayers mimicking different types of membrane domains (Fig.5). The lipid compositions used (table 1) for l_d and l_o phase correspond to ends of the same tie-line in the phase diagram, in order to ensure their possible coexistence in a phase separated mixture, i.e., a raft-containing membrane model [36]. As expected, in the control samples the steady state fluorescence anisotropy decreases in the order gel > l_o > l_d, with values similar to those previously reported for the gel phase (> 0.3), l_o (0.2 - 0.3), and l_d (< 0.2) [36, 38] (Fig. 5A). Regarding *t*-PnA mean fluorescence lifetime, control values were as expected above 30 ns for gel phase, ~20 ns for l_o and ~10 ns for l_d (Fig. 5B). With the addition of any 2OHFA, both DPH steady state fluorescence anisotropy and *t*-PnA mean fluorescence lifetime values diminished, pointing towards membrane fluidification with a looser packing of the acyl chains (Fig. 5A-B). Furthermore, di-4-ANEPPS steady state fluorescence anisotropy also decreased, meaning that the probe has a faster and/or less restrained rotational dynamics, indicating that 2-OHFA induce a less tight packing in the lipid headgroup region of the bilayer (Fig. 5C). In fact, the trend observed for di-4-ANEPPS fluorescence anisotropy (Fig. 5C) is parallel to those of DPH (Fig. 5A) and *t*-PnA (Fig. 5B). The results show a similar tendency towards membrane order changes with the three probes tested (DPH – Fig.5 A; *t*-PnA – Fig.5 B;

di-4-ANEPPS – Fig.5 C) independently of the lipid phase, with a greater effect observed for 2OHARA then for either 2OHDHA or 2OHOA. Interestingly, l_o was the least affected type of membrane phase by any of the different 2OHFA derivatives.

This disordering effect is also accompanied with changes of hydration state, solvent relaxation dynamics and dipole potential. This is evidenced by both shorter fluorescence lifetimes of di-4-ANEPPS in l_d and l_o membranes (not shown), and spectral red-shifts of emission of di-4-ANEPPS dye for the three phases that will be described below (Table 3) which are due to a stronger contact of the probe with polar water molecules. Regarding the fluorescence lifetimes, an exceptional behavior was observed for gel phase LUVs, which are formed by a single lipid, SM. In this type of phase it is well known that line defects exist, which are analogous to crystal grain boundaries, and are able to accumulate "impurities" due to their increased hydration [55, 56]. As it can be observed in Fig. 5D, di-4-ANEPPS excited state mean fluorescence lifetime becomes longer in the presence of the 2OHFA, with a more pronounced effect for 2OHDHA. This exceptional behavior can be explained by fatty acids preference for the line defects (. An occupation of those defects would reduce the hydration, thereby increasing di-4-ANEPPS fluorescence lifetime. This is consistent with the order in which the effect is observed. 2OHOA has the acyl chain that is more similar to the egg SM acyl chain and sphingoid base length [57], and therefore should be the one who can accommodate better in non-defect regions. On the contrary, 2OHDHA, having the longer acyl chain and the highest number of unsaturations, should have the opposite behavior, showing an extensive preference for the defects, and thus the larger effect in reducing hydration of the gel phase. In fact, for DHA, several conformations are predicted, and for those with most extreme bending it is not expected that they easily accommodate between the phospholipid acyl chains [14].

In the three types of lamellar lipid phases relevant for animal cell membranes and in the situation of l_d / l_o coexistence (quaternary mixture) the membrane alterations induced by the fatty acids corresponded to a decrease in the order/compactness and increased hydration of the membrane (except for the single gel phase situation). The effects were always more marked for 2OHARA than 2OHDHA and 2OHOA. Therefore, our results suggest that the fatty acids have

the ability to interact with the three types of lipid domains when having their first contact with the target cell membrane. Moreover, this general disordering effect is expected to contribute to remixing of the lipids between ordered and disordered domains. The preference shown for the line defects of the gel phase suggests that, as already known for a large number of small amphiphilic molecules, they may somehow prefer to incorporate in membrane defects that are more likely to be present at the interfaces between ordered and disordered domains, reducing line tension between them and leading to smaller / less well defined areas. This last feature was indeed recently observed on GUV [13].

Interaction with liquid ordered domains and l_d / l_o *phase coexistence mixtures* – In both quaternary mixtures used in this work there is coexistence of l_d and l_o phases, as observed by confocal microscopy in GUVs[13] and predicted by mapping their composition on an experimentally determined phase diagram[7]. In this case the probes DPH and t-PnA were used due to the fact that they have l_d / l_o partition coefficients close to one in a variety of binary and ternary Chol-containing mixtures [58, 59].Therefore, the changes undergone in DPH anisotropy and in t-PnA mean fluorescence lifetime can be interpreted straightforward as alterations in phase properties and proportion, and are not affected by possible changes in probe partition behavior. Interestingly, the fluidizing effect of 2OHFA is very weak in the l_o phase (Fig. 5A-C, grey bars), which could explain the low amplitude of the effect on DPH steady state anisotropy in the equimolar quaternary mixture (Fig. 4A). The control value in this mixture is near the upper limit for an l_o phase, implying a high proportion of l_o phase in the phase coexisting mixture as also observed in GUVs[13]. On the other hand, in liposomes mimicking U-118 glioma cell membrane (table 1), the fluidizing effect of the 2OHFA, particularly 2OHARA, was much more pronounced (Fig. 6). For this composition, the values of the control were lower than for the equimolar system, regarding both DPH anisotropy (Fig. 6A) and *t*-PnA fluorescence lifetime (Fig. 6B), which indicates a smaller proportion of l_o phase than for the equimolar mixture, in agreement with the prediction carried out by mapping such composition in the phase diagram[7]. This lower proportion of l_o phase justifies, to a large extent, the more marked effects of 2OHOA when compared to those in the equimolar mixture. Moreover, the significantly smaller amount of SM (Table 1) should

correspond to a higher preponderance of nanometer rather than micrometer-sized domains [38], which would correspond to a larger fraction of lipids in the l_d / l_o domain interfaces. Finally, the effect on U-118 model membrane systems was larger than for both l_o and l_d phases separately (Fig. 5), suggesting that l_d / l_o phase coexistence has a role in the initial interaction of 2OHFA with the membrane. For example, upon addition of 2OHARA the anisotropy of DPH is decreased by ~35% in U-118 cell membranes models, whereas the decrease was only ~20% in l_d membranes and not significant in l_o. Using t-PnA mean fluorescence lifetime, similar conclusions can be reached. Thus the changes observed in the single phase systems cannot account for the extent of the alterations observed for l_d / l_o coexistence, showing that the presence of two phases enhances the effects of 2OHARA. The compositions of the pure l_d and pure l_o phases were chosen to be extremes of the same tie-line. Therefore, if phase coexistence enhances the effects observed, this must be related with domain size and the presence of domain boundaries, which are the distinctive features of the l_d / l_o coexistence situation when compared to a linear combination of the properties obtained in the pure phases.

Di-4-ANEPPS is an environmentally sensitive probe particularly adequate to investigate the effects of Chol, and this probe was used to further access the possible role of lipid rafts in 2OHFA interaction with model membranes in each of the three main lamellar phases (l_d, l_o and gel). The excitation and emission spectra of di-4-ANEPPS (Table 3 and Fig. S2) were analyzed and it was observed that the effects on hydration patterns at the lipid-water interface induced by the 2OHFA were much larger for the l_o phase than for the others. This contrasts with the effects observed on DPH steady state fluorescence anisotropy and *t*-PnA fluorescence mean lifetime data, suggesting a possible role of Chol (or lipid rafts). Chol induces a strong blue-shift of di-4-ANEPPS fluorescence emission, due to the reduced hydration and change of solvent relaxation dynamics, accompanied by a reorientation of the phospholipids headgroup or surrounding water molecules and therefore reorganization of the H-bonding patterns in presence of Chol [37]. However, upon incubation with 2OHFA the extent of the shift is significantly reduced. In case of 2OHARA, this effect is so strong that the wavelength of maximum emission becomes the same as the one observed for the l_d and gel membranes, i.e., in those membranes that contain as few as 5 mol%

cholesterol, or do not contain sterol at all, respectively (Table 3). Thus, the consequence of 2OHFA incorporation into the membranes is not restricted to a disordering of the acyl chains, but it also affects significantly hydration and solvent relaxation dynamics.

The excitation spectra of di-4-ANEPPS also contain information on the membrane dipole potential, a feature that is significantly enhanced by certain sterols, namely Chol. This biophysical property can be expressed as a ratio of excitation intensity at two wavelengths, which was calculated and is shown in Fig. 7. The ratio of intensities is a suitable way of representing dipole potential alterations, because there is a close to linear relation between them, and also because the use of a ratio amplifies the range of possible values when compared to single-wavelength measurements, and is therefore a much more sensitive parameter. Fig. 7 shows that the membrane dipole potential was decreased upon FA insertion into the bilayer. The effect was stronger for 2OHARA than 2OHDHA and 2OHOA and its magnitude increased in the order gel> l_d> l_o. In the case of 2OHARA and l_o phase, the dipole potential decreased to values measured in the liposomes devoid of Chol, i.e., in the gel phase, suggesting that it able to override the sterol-induced dipole potential. Again, it is shown that in the l_o phase the general disordering effect is small, but significant changes of other biophysical properties occur upon insertion of the 2OHFA. The alterations observed in the interfacial region hydration patterns and dipole potential indicate that l_o phase become much more similar to the other phases in terms of these properties. In addition, it justifies once more the intermixing of l_d and l_o structures producing smaller microdomains, as previously observed in GUVs [13].

Membrane incorporation versus lipid bilayer order effect of 2OHFA- The overall membrane effects of 2OHFAs on membrane order are not related to their incorporation ability, as 2OHDHA, the 2-hydroxylated molecule with the highest membrane affinity (Table 2) showed the lowest effect on membrane domain remodeling. On the other hand, 2OHARA has a greater effect on the membrane lipid order than 2OHOA, but both share a Kd with the same order of magnitude. A smaller disordering effect of 2OHOA is consistent with the changes induced on membrane elastic properties of their non-hydroxylated counterparts [16]. Based on previous studies of OHFA effect on DMPC model membranes, the general disordering effect of the 2OHFA in the present work

can be primarily attributed to the unsaturation of the acyl chain, as the 2OH group was shown to stabilize the gel phase, increasing the T_m of DMPC [28]. The smaller disorganizing effect of 2OHDHA can be explained by its longer acyl chain in comparison with the other 2OHFA, which opposes the disordering effect of the greater number of double bonds. In addition, and as mentioned above, highly bended conformations of 2OHDHA (by analogy to DHA; [14]) may adsorb more superficially to the lipid bilayer, and only a fraction will penetrate into the acyl chain region. On the other hand, 2OHARA penetrates more easily into the lipid bilayer and its polyunsaturation will have a strong disordering effect.

When analyzing the consequences of lipid composition changes in U-118 cells treated with 2OHOA, it was shown that 2OHOA increases the order of the l_o domains in membrane models and reconstituted liposomes due to accumulation of SM in 2OHOA treated cells [7]. When the direct effect of 2OHOA insertion was evaluated without taking into account the changes in lipid composition due to lipid metabolism alterations, a small disordering effect was observed, and the values retrieved for both DPH fluorescence anisotropy and *t*-PnA mean fluorescence lifetime [30] fit in the general trend presented here for the three 2OHFA. We demonstrate here that the disorganization effect due to 2OHFA also occurs in quaternary lipid mixtures used as a model of mammalian plasma membrane and in LUVs with compositions corresponding to different lipid phases, showing that this is a general effect of the unsaturated 2OHFA.

The decrease in the order/compactness of the phospholipid acyl chains due to 2OHFA incorporation, more obvious in gel and l_d phase membranes is also accompanied by a decrease in the membrane dipole potential, and increased hydration of the membrane, these latter effects being more noticeable for the membranes in the l_o phase, followed by l_d, i.e. for Chol-containing membranes. Previous studies of X-ray scattering patterns and DSC heating thermograms have also pointed to an increased hydration and membrane fluidity due to 2OHOA incorporation in phase coexisting mixtures (DOPC:SM:Chol; 35:35:30 mol ratio) [29]. Our results also show that with the exception of the gel phase hydration which decreases, in all cases, there is an increased water penetration and reorientation of water molecules at the membrane/water interface, as

evidenced from the emission red shift provoked by the 2OHFA and alterations of membrane dipole potential (Table 3).

The role of lipid lateral organization on membrane – 2OHFA interactions - Our results also suggest an important role for lipid domains, as 2OHFA effect in the l_d / l_o phase coexistence system is overall larger than for l_o and l_d phases separately. Indeed, the comparison of the data in Fig. 5 and Fig. 6 indicates that the phase coexistence is enhancing the effect of the 2OHFA. Interestingly, in case of the gel phase the effects are more marked and more similar to the quaternary mixtures, which may indicate that gel grain boundaries in one case, and l_d / l_o domain boundaries in the other, are important for the interaction. This suggests that phase coexistence has an important role in the initial interaction of 2OHFA with the membrane, especially for 2OHARA. The difference between the amplitude of membrane disordering effect in the equimolar and U-118 phase coexisting mixtures can be explained by a higher l_o proportion in the former. The fact that the 2OHFA exert changes of different magnitude in these two model systems suggests that the lipid composition and membrane microdomain organization of a given cell type might be relevant for the mechanism of action of the FA in that particular cell type. This would partially explain the observation of different anti-cancer mechanisms (cell cycle arrest, differentiation, and apoptosis) for 2OHOA when using different cell lines [6, 7].

The effect of direct incorporation of 2OHFA in the global order of the membrane (DPH steady state fluorescence anisotropy) is almost imperceptible in l_o phase (Fig. 5A), which could point to a lack of effect in this phase. Nevertheless, further analysis of the model systems labeled with di-4-ANEPPS has shown that 2OHARA, especially affects Chol-rich domains (l_o), overriding Chol effect on hydration and H-bonding patterns and membrane dipole potential. As previously hypothesized [13], this result supports the idea that the fatty acids interact with phospholipids/sphingolipids, diminishing their interaction with Chol, which can widely affect the molecular interactions within lipid rafts.. The results of the present studygive support to the notion that by competing for hydrogen bonding with the sphingolipid headgroup, the 2-OHFA will strongly affect sterol/sphingolipid interactions which are responsible for certain particular features of the l_o phase, such has a large dipole potential, which was seen here to be reduced in

the case of 2-OHARA to the same level as in membranes devoid of Chol. Moreover, the establishment of H-bonding with a different molecule explains the changes in H-bonding patterns revealed by the spectral shifts in di-4-ANEPPS emission, which are also much stronger for the membranes in the l_o phase than in either l_d or gel membranes.

CONCLUDING REMARKS

The present study aimed at the understanding of the biophysical effects of 2OHFA in lipid bilayer membranes. To this purpose, different biophysical techniques and model systems were employed. Overall the results show that 2OHFA are able to interact spontaneously with the membrane and reorganize the lipid bilayer microdomains, in an affinity and, to a certain extent, phase independent manner.

The FA and 2OHFA incorporation into the membrane bilayer occurs spontaneously up to Π values ~40 mN/m, above the standard Π values of a cell membrane (~30 mN/m). This result becomes a direct proof of insertion of 2OHFA and FA into lipid model membranes, and suggesting a similar behavior in living cells. The incorporation of FA and 2OHFA occurs above critical micellar concentrations, which is important, for instance, to understand cellular effects of these compounds, since typical concentrations for cell treatment are in the tenths of μM, attaining levels of 200 μM.

Thus, we demonstrate that 2OHFA incorporation affect the biophysical properties of the membrane. The strong changes induced by 2OHARA in membrane organization, hydration and dipole potential suggest that in opposition to the other 2OHFA studied, the initial interaction with the membrane and the domain reorganization might be an important step of its mechanism of action.

ACKNOWLEDGEMENTS

The authors thank Dr. Gwendolyn Barceló-Coblijn from University of the Balearic Islands for the help provided during the elaboration of the manuscript and Dr. Jesús Sot and Dr. Itziar Martínez from the University of the Basque Country for their assistance in the surface pressure experiments.

This work was supported by grants from Fundación Marathon (PVE), by Grants to Research Groups of Excellence from Govern de les Illes Balears (PVE) and Spanish Ministerio de Ciencia e Innovación grants BIO2010-21132, PTQ-10-04214 (MI) and PTQ-09-02-02113 (DJL). This work was also financed by Portuguese national funds and Fundo Social Europeu through FCT, the Portuguese Foundation for Science and Technology, by "Ciência 2007" and "Investigador FCT 2012" Initiatives (POPH), by grant PEst-OE/QUI/UI0612/2011-2013. A.K. acknowledges a scholarship from Fundação Amadeu Dias/Universidade de Lisboa.

Supporting Information Available

Additional data is presented online as Supporting Information: Figure S1 - Determination of oxidation of FA or 2OHFA; Figure S2 - Di-4-ANEPSS normalized excitation and emission spectra in gel, l_d and l_o single-phase membranes, control and in the presence of 2OHFA. This information is available free of charge via the Internet at http://pubs.acs.org/.

Conflict of interest. M.I. and D.J.L. were supported by Torres-Quevedo Research Contracts granted to Lipopharma Therapeutics, S.L. by Ministerio de Economía y Competitividad. Lipopharma Therapeutics, S.L. is a spin-off, pharmaceutical company from the University of the Balearic Islands.

Footnotes

‡Both authors contributed equally to this work.

*Corresponding authors: Rodrigo F.M de Almeida (rodrigo.almeida@fc.ul.pt), David J. López (davidlopez_95@hotmail.com)

Abbreviations

Π, surface pressure; 2OHARA, 2-hydroxyarachidonic acid; 2OHDHA, 2-hydroxy-docosahexaenoic acid; 2OHEPA, 2-hydroxyeicosapentaenoic acid; 2OHFA, 2-hydroxy fatty acid; 2OHOA, 2-hydroxyoleic acid; ARA, arachidonic acid; Chol, cholesterol; DHA, docosahexaenoic acid; di-4-ANEPPS, 4-(2-(6-(dibutylamino)-2-naphthalenyl)ethenyl)-1-(3-

sulfopropyl)pyridinium hydroxide inner salt; DMSO, dimetil sulfoxide; DPH, 1,6-diphenol-1,3,5-hexatriene; EPA, eicosapentaenoic acid; GUV, giant unilamellar vesicle; ITC, isothermal titration calorimetry; l_d, liquid-disordered; l_o, liquid-ordered; LUV, large unilamellar vesicle; OA, oleic acid; PE, phosphatidylethanolamine; POPC, 1-palmitoyl-2-oleoyl-*sn*-glycero-3-phosphatidylcholine; SM, sphingomyelin; *t*-PnA, *trans*-parinaric acid.

REFERENCES

1. Barceló, F.; Perona, J. S.; Prades, J.; Funari, S. S.; Gómez-Gracia, E.; Conde, M.; Estruch, R.; Ruiz-Gutiérrez, V. Mediterranean-style diet effect on the structural properties of the erythrocyte cell membrane of hypertensive patients: the Prevencion con Dieta Mediterranea Study. *Hypertension* **2009,** *54* (5), 1143-50.

2. Carrillo, C.; Cavia Mdel, M.; Alonso-Torre, S. Role of oleic acid in immune system; mechanism of action; a review. *Nutr Hosp* **2012,** *27* (4), 978-90.

3. Lavie, C. J.; Milani, R. V.; Mehra, M. R.; Ventura, H. O. Omega-3 polyunsaturated fatty acids and cardiovascular diseases. *J Am Coll Cardiol* **2009,** *54* (7), 585-94.

4. Lukiw, W. J.; Cui, J. G.; Marcheselli, V. L.; Bodker, M.; Botkjaer, A.; Gotlinger, K.; Serhan, C. N.; Bazan, N. G. A role for docosahexaenoic acid-derived neuroprotectin D1 in neural cell survival and Alzheimer disease. *J Clin Invest* **2005,** *115* (10), 2774-83.

5. Alemany, R.; Vögler, O.; Terés, S.; Egea, C.; Baamonde, C.; Barceló, F.; Delgado, C.; Jakobs, K. H.; Escribá, P. V. Antihypertensive action of 2-hydroxyoleic acid in SHRs via modulation of the protein kinase A pathway and Rho kinase. *J Lipid Res* **2006,** *47* (8), 1762-70.

6. Lladó, V.; Gutiérrez, A.; Martínez, J.; Casas, J.; Terés, S.; Higuera, M.; Galmes, A.; Saus, C.; Besalduch, J.; Busquets, X.; Escribá, P. V. Minerval Induces Apoptosis In Jurkat And Other Cancer Cells. *J Cell Mol Med* **2008**.

7. Barceló-Coblijn, G.; Martin, M. L.; de Almeida, R. F.; Noguera-Salva, M. A.; Marcilla-Etxenike, A.; Guardiola-Serrano, F.; Luth, A.; Kleuser, B.; Halver, J. E.; Escribá, P. V. Sphingomyelin and sphingomyelin synthase (SMS) in the malignant transformation of glioma cells and in 2-hydroxyoleic acid therapy. *Proc Natl Acad Sci* **2011,** *108* (49), 19569-74.

8. López, D. H.; Fiol-Deroque, M. A.; Noguera-Salva, M. A.; Terés, S.; Campana, F.; Piotto, S.; Castro, J. A.; Mohaibes, R. J.; Escribá, P. V.; Busquets, X. 2-hydroxy arachidonic Acid: a new non-steroidal anti-inflammatory drug. *PloS one* **2013,** *8* (8), e72052.

9. Vögler, O.; Barceló, J. M.; Ribas, C.; Escribá, P. V. Membrane interactions of G proteins and other related proteins. *Biochim Biophys Acta* **2008,** *1778* (7-8), 1640-52.

10. Fiol-Deroque, M. A.; Gutiérrez-Lanza, R.; Terés, S.; Torres, M.; Barceló, P.; Rial, R. V.; Verkhratsky, A.; Escribá, P. V.; Busquets, X.; Rodríguez, J. J. Cognitive recovery and restoration of cell proliferation in the dentate gyrus in the 5XFAD transgenic mice model of Alzheimer's disease following 2-hydroxy-DHA treatment. *Biogerontology* **2013,** 14 (6), 763-75.

11. Pfleger, R. C.; Anderson, N. G.; Snyder, F. Lipid class and fatty acid composition of rat liver plasma membranes isolated by zonal centrifugation. *Biochemistry* **1968,** *7* (8), 2826-33.

12. Waheed, A. A.; Yasuzumi, F.; Gupta, P. D. Lipid and fatty acid composition of brush border membrane of rat intestine during starvation. *Lipids* **1998,** *33* (11), 1093-7.

13. Ibarguren, M.; López, D. J.; Encinar, J. A.; González-Ros, J. M.; Busquets, X.; Escribá, P. V. Partitioning of liquid-ordered/liquid-disordered membrane microdomains induced by the fluidifying effect of 2-hydroxylated fatty acid derivatives. *Biochim Biophys Acta* **2013,** *1828* (11), 2553-63.

14. Stillwell, W. The role of polyunsaturated lipids in membrane raft function. *Scandinavian Journal of Food and Nutrition* **2006,** *50 (S2)*, 107-113.

15. Leaf, A.; Xiao, Y. F. The modulation of ionic currents in excitable tissues by n-3 polyunsaturated fatty acids. *J Membr Biol* **2001,** *184* (3), 263-71.

16. Bruno, M. J.; Koeppe, R. E., 2nd; Andersen, O. S. Docosahexaenoic acid alters bilayer elastic properties. *Proc Natl Acad Sci U S A* **2007,** *104* (23), 9638-43.

17. Fernandez Nievas, G. A.; Barrantes, F. J.; Antollini, S. S. Modulation of nicotinic acetylcholine receptor conformational state by free fatty acids and steroids. *The Journal of biological chemistry* **2008,** *283* (31), 21478-86.

18. López, D. J.; Egido-Gabas, M.; López-Montero, I.; Busto, J. V.; Casas, J.; Garnier, M.; Monroy, F.; Larijani, B.; Goñi, F. M.; Alonso, A. Accumulated Bending Energy Elicits Neutral Sphingomyelinase Activity in Human Red Blood Cells. *Biophysical journal* **2012,** *102* (9), 2077-2085.

19. Lenaz, G. Lipid fluidity and membrane protein dynamics. *Biosci Rep* **1987,** *7* (11), 823-37.

20. Uchida, Y.; Hama, H.; Alderson, N. L.; Douangpanya, S.; Wang, Y.; Crumrine, D. A.; Elias, P. M.; Holleran, W. M. Fatty acid 2-hydroxylase, encoded by FA2H, accounts for differentiation-associated increase in 2-OH ceramides during keratinocyte differentiation. *The Journal of biological chemistry* **2007,** *282* (18), 13211-9.

21. Zoller, I.; Meixner, M.; Hartmann, D.; Bussow, H.; Meyer, R.; Gieselmann, V.; Eckhardt, M. Absence of 2-hydroxylated sphingolipids is compatible with normal neural development but causes late-onset axon and myelin sheath degeneration. *The Journal of neuroscience : the official journal of the Society for Neuroscience* **2008,** *28* (39), 9741-54.

22. Guo, L.; Zhou, D.; Pryse, K. M.; Okunade, A. L.; Su, X. Fatty acid 2-hydroxylase mediates diffusional mobility of Raft-associated lipids, GLUT4 level, and lipogenesis in 3T3-L1 adipocytes. *The Journal of biological chemistry* **2010,** *285* (33), 25438-47.

23. Filippov, A.; Oradd, G.; Lindblom, G. Domain formation in model membranes studied by pulsed-field gradient-NMR: the role of lipid polyunsaturation. *Biophysical journal* **2007,** *93* (9), 3182-90.

24. Schley, P. D.; Brindley, D. N.; Field, C. J. (n-3) PUFA alter raft lipid composition and decrease epidermal growth factor receptor levels in lipid rafts of human breast cancer cells. *J Nutr* **2007,** *137* (3), 548-53.

25. Shaikh, S. R.; Rockett, B. D.; Salameh, M.; Carraway, K. Docosahexaenoic acid modifies the clustering and size of lipid rafts and the lateral organization and surface expression of MHC class I of EL4 cells. *J Nutr* **2009,** *139* (9), 1632-9.

26. Simonsen, A. C. Activation of phospholipase A2 by ternary model membranes. *Biophysical journal* **2008,** *94* (10), 3966-75.

27. Leidy, C.; Ocampo, J.; Duelund, L.; Mouritsen, O. G.; Jorgensen, K.; Peters, G. H. Membrane restructuring by phospholipase A2 is regulated by the presence of lipid domains. *Biophysical journal* **2011,** *101* (1), 90-9.

28. Jenske, R.; Lindstrom, F.; Grobner, G.; Vetter, W. Impact of free hydroxylated and methyl-branched fatty acids on the organization of lipid membranes. *Chemistry and physics of lipids* **2008,** *154* (1), 26-32.

29. Prades, J.; Funari, S. S.; Gómez-Florit, M.; Vögler, O.; Barceló, F. Effect of a 2-hydroxylated fatty acid on Cholesterol-rich membrane domains. *Mol Membr Biol* **2012**.

30. Martin, M. L.; Barceló-Coblijn, G.; de Almeida, R. F.; Noguera-Salva, M. A.; Terés, S.; Higuera, M.; Liebisch, G.; Schmitz, G.; Busquets, X.; Escribá, P. V. The role of membrane fatty acid remodeling in the antitumor mechanism of action of 2-hydroxyoleic acid. *Biochim Biophys Acta* **2013,** *1828* (5), 1405-13.

31. Cerezo, J.; Zúñiga, J.; Bastida, A.; Requena, A.; Cerón-Carrasco, J. P. Atomistic molecular dynamics simulations of the interactions of oleic and 2-hydroxyoleic acids with phosphatidylcholine bilayers. *The journal of physical chemistry. B* **2011,** *115* (40), 11727-38.

32. Aresta-Branco, F.; Cordeiro, A. M.; Marinho, H. S.; Cyrne, L.; Antunes, F.; de Almeida, R. F. Gel domains in the plasma membrane of Saccharomyces cerevisiae: highly ordered, ergosterol-free, and sphingolipid-enriched lipid rafts. *The Journal of biological chemistry* **2011,** *286* (7), 5043-54.

33. Jaikishan, S.; Slotte, J. P. Stabilization of sphingomyelin interactions by interfacial hydroxyls - a study of phytosphingomyelin properties. *Biochim Biophys Acta* **2013,** *1828* (2), 391-7.

34. Penalva, D. A.; Furland, N. E.; Lopez, G. H.; Aveldano, M. I.; Antollini, S. S. Unique thermal behavior of sphingomyelin species with nonhydroxy and 2-hydroxy very-long-chain (C28-C32) PUFAs. *J Lipid Res* **2013,** *54* (8), 2225-35.

35. Mayer, L. D.; Hope, M. J.; Cullis, P. R. Vesicles of variable sizes produced by a rapid extrusion procedure. *Biochim Biophys Acta* **1986,** *858* (1), 161-8.

36. de Almeida, R. F.; Fedorov, A.; Prieto, M. Sphingomyelin/phosphatidylcholine/cholesterol phase diagram: boundaries and composition of lipid rafts. *Biophysical journal* **2003,** *85* (4), 2406-16.

37. Bastos, A. E.; Marinho, H. S.; Cordeiro, A. M.; de Soure, A. M.; de Almeida, R. F. Biophysical properties of ergosterol-enriched lipid rafts in yeast and tools for their study: characterization of ergosterol/phosphatidylcholine membranes with three fluorescent membrane probes. *Chemistry and physics of lipids* **2012,** *165* (5), 577-88.

38. de Almeida, R. F.; Loura, L. M.; Fedorov, A.; Prieto, M. Lipid rafts have different sizes depending on membrane composition: a time-resolved fluorescence resonance energy transfer study. *J Mol Biol* **2005,** *346* (4), 1109-20.

39. Barry, J. A.; Gawrisch, K. Effects of ethanol on lipid bilayers containing cholesterol, gangliosides, and sphingomyelin. *Biochemistry* **1995,** *34* (27), 8852-60.

40. Calvez, P.; Bussieres, S.; Eric, D.; Salesse, C. Parameters modulating the maximum insertion pressure of proteins and peptides in lipid monolayers. *Biochimie* **2009,** *91* (6), 718-33.

41. Arregi, I.; Falces, J.; Banuelos, S.; Urbaneja, M. A.; Taneva, S. G. The nuclear transport machinery recognizes nucleoplasmin-histone complexes. *Biochemistry* **2011,** *50* (33), 7104-10.

42. Loch, J. I.; Bonarek, P.; Polit, A.; Ries, D.; Dziedzicka-Wasylewska, M.; Lewinski, K. Binding of 18-carbon unsaturated fatty acids to bovine beta-lactoglobulin--structural and thermodynamic studies. *International journal of biological macromolecules* **2013,** *57*, 226-31.

43. Haldar, S.; Kanaparthi, R. K.; Samanta, A.; Chattopadhyay, A. Differential effect of cholesterol and its biosynthetic precursors on membrane dipole potential. *Biophysical journal* **2012,** *102* (7), 1561-9.

44. Lakowics, J. R. *Principles of Fluorescence Microscopy, 3rd edition. Springer*. **2006**.

45. Schnitzer, E.; Pinchuk, I.; Bor, A.; Fainaru, M.; Samuni, A. M.; Lichtenberg, D. Lipid oxidation in unfractionated serum and plasma. *Chemistry and physics of lipids* **1998,** *92* (2), 151-70.

46. Clint, J. Micellization of mixed nonionic surface active agents. *Journal of the Chemical Society, Faraday Transactions 1: Physical Chemistry in Condensed Phases* **1975,** *71*, 1327-1334.

47. Peltonen, L. J.; Yliruusi, J. Surface Pressure, Hysteresis, Interfacial Tension, and CMC of Four Sorbitan Monoesters at Water-Air, Water-Hexane, and Hexane-Air Interfaces. *Journal of colloid and interface science* **2000,** *227* (1), 1-6.

48. García-Pacios, M.; Collado, M. I.; Busto, J. V.; Sot, J.; Alonso, A.; Arrondo, J. L.; Goñi, F. M. Sphingosine-1-phosphate as an amphipathic metabolite: its properties in aqueous and membrane environments. *Biophysical journal* **2009,** *97* (5), 1398-407.

49. Marsh, D. Lateral pressure in membranes. *Biochim Biophys Acta* **1996,** *1286* (3), 183-223.

50. Anel, A.; Richieri, G. V.; Kleinfeld, A. M. Membrane partition of fatty acids and inhibition of T cell function. *Biochemistry* **1993,** *32* (2), 530-6.

51. Lentz, B. R. Use of fluorescent probes to monitor molecular order and motions within liposome bilayers. *Chemistry and physics of lipids* **1993,** *64* (1-3), 99-116.

52. Sklar, L. A.; Hudson, B. S.; Simoni, R. D. Conjugated polyene fatty acids as fluorescent probes: synthetic phospholipid membrane studies. *Biochemistry* **1977,** *16* (5), 819-28.

53. Loew, L. M. Potentiometric dyes: imaging electrical activity of cell membranes. . *Pure & Appl Chem* **1996,** *68* (1405-9).

54. Asawakarn, T.; Cladera, J.; O'Shea, P. Effects of the membrane dipole potential on the interaction of saquinavir with phospholipid membranes and plasma membrane receptors of Caco-2 cells. *The Journal of biological chemistry* **2001,** *276* (42), 38457-63.

55. Keller, D.; Larsen, N. B.; Moller, I. M.; Mouritsen, O. G. Decoupled phase transitions and grain-boundary melting in supported phospholipid bilayers. *Phys Rev Lett* **2005,** *94* (2), 025701.

56. Yarrow, F.; Kuipers, B. W. AFM study of the thermotropic behaviour of supported DPPC bilayers with and without the model peptide WALP23. *Chemistry and physics of lipids* **2011,** *164* (1), 9-15.

57. Marsh, D. *Handbook of lipid bilayers*; CRC Press: Boca Raton, FL, 2013.

58. de Almeida, R. F.; Loura, L. M.; Prieto, M. Membrane lipid domains and rafts: current applications of fluorescence lifetime spectroscopy and imaging. *Chemistry and physics of lipids* **2009,** *157* (2), 61-77.

59. Nyholm, T. K.; Lindroos, D.; Westerlund, B.; Slotte, J. P. Construction of a DOPC/PSM/cholesterol phase diagram based on the fluorescence properties of trans-parinaric acid. *Langmuir : the ACS journal of surfaces and colloids* **2011,** *27* (13), 8339-50.

Table 1: Mole fraction of the lipids used to mimic the lipid composition of the mammalian plasma membrane, U-118 cells plasma membrane[7] and the main types of lipid phases[36].

	mole %				
	Mammalian plasma membrane model	U-118 glioma cell membrane	l_d	l_o	gel
POPC	25.0	36.2	71.8	25.2	-
POPE	25.0	23.6	-	-	-
PSM	25.0	6.8	23.1	35.5	100
Cholesterol	25.0	33.4	5.1	39.3	-

Table 2 Thermodynamic parameters for FA and 2OHFA-membrane interaction obtained from isothermal titration calorimetry using LUVs composed of POPC:SM:PE:Chol (1:1:1:1; mol ratio).

Fatty acid	Kd (μM)	ΔHº(Kcal/mol)	-TΔSº(Kcal/mol)	ΔGº (Kcal/mol)
OA	3.65 ± 0.18	-3.09 ± 0.01	-4.32 ± 0.03	-7.41 ± 0.04
2OHOA	28.92 ± 3.02**	-1.46 ± 0.4**	-4.79 ± 0.41	-6.22 ± 0.01***
ARA	49.38 ± 11.5	-1.62 ± 0.5	-4.89 ± 0.36	-5.7 ± 0.28
2OHARA	27.86 ± 7.5	-3.43 ± 0.65	-3.85 ± 0.25	-7.28 ± 0.9
DHA	39.24 ± 5.8	-5.0 ± 0.92	-1.89 ± 0.4	-6.89 ± 1.3
2OHDHA	4.37 ± 2.86**	-3.99 ± 0.19	-3.48 ± 0.27*	-7.47 ± 0.46

Mean value ± S.D. Statistics comparing the FA with the 2OHFA* p <0.05, ** <0.01 and *** <0.001.

Table 3 Di-4-ANEPPS (probe/lipid ratio 1/500) excitation and emission spectral maxima wavelengths in liposomes with compositions corresponding to a single gel, l_d or l_o phase with compositions given in Table 1, and spectral shifts induced by the 2-hydroxylated fatty acids.

	Gel		l_o		l_d	
	λ_{ex}(max)	λ_{em}(max)	λ_{ex}(max)	λ_{em}(max)	λ_{ex}(max)	λ_{em}(max)
Control	475	622	462	582	468	618
2OHOA	477	624	472	597	472	618
2OHARA	484	617	481	622	476	621
2OHDHA	481	618	472	597	467	618

.

FIGURE LEGENDS

FIGURE 1. Chemical structures of the natural and synthetic fatty acids used in the study. OA, oleic acid (C18:1); ARA, arachidonic acid (C20:4); DHA, docosahexaenoic acid (C22:6); 2OHOA, 2-hydroxyoleic acid (C18:1); 2OHARA, 2-hydroxyarachidonic acid (C20:4) and 2OHDHA, 2-hydroxydocosahexaenoic acid (C22:6).

FIGURE 2. Surface pressure measurements of FA or 2OHFA in model membranes. **(A-C)** Tensioactive properties of **(A)** OA or 2OHOA, **(B)** ARA or 2OHARA and **(C)** DHA or 2OHDHA. The increase of Π in the buffer-air interphase was recorded at increasing concentrations of natural and hydroxylated FAs injected in the subphase. **(D-F)** Insertion of 30 μM FA or 2OHFAs into phospholipid monolayers composed of POPC:SM:PE:Chol (1:1:1:1; mol ratio). Changes in Π induced by **(D)** OA or 2OHOA, **(E)** ARA or 2OHARA and **(F)** DHA or 2OHDHA were plotted against the Π_i values of the pre-formed phospholipid monolayer. Naturally occurring fatty acids (OA, ARA, DHA) are shown as filled squares while synthetic, 2-hydroxylated fatty acids (2OHOA, 2OHARA, 2OHDHA) are represented by filled circles. Data represent mean values ± SD of three independent experiments.

FIGURE 3. Isothermal Titration Calorimetry assay of binding of 2OHOA to LUV composed of POPC:PE:SM:Chol (1:1:1:1; mol ratio). **(A)** Representative titration experiment of LUV (10 mM) and 2OHOA (30 μM) and **(B)** integrated data (■) and one-site fitting curve of the binding isotherm from panel A.

FIGURE 4. Fluorescence spectroscopy analysis of liposomes composed of POPC: POPE: SM: Chol(1:1:1:1; mol ratio) incubated with 2-hydroxylated fatty acids. **(A)** DPH steady state fluorescence anisotropy (3 nm bandwidth) and **(B)** *t*-PnA mean fluorescence lifetime. Statistics comparing the control with the 2OHFA treated sample: * p <0.05, ** <0.01 and *** <0.001.

FIGURE 5. Fluorescence spectroscopy analysis of membrane order and compactness in lipid vesicles with compositions corresponding to a single phase, gel (filled bars), l_o (grey bars) or l_d (empty bars), as described in Table 1, incubated with 2-hydroxylated fatty acids. **(A)** DPH steady

state fluorescence anisotropy (3 nm bandwidth). **(B)** *t*-PnA mean fluorescence lifetime. **(C)** Di-4-ANEPPS steady state fluorescence anisotropy (4 nm bandwidth). **(D)** Di-4-ANEPSS mean fluorescence lifetime in liposomes of SM in the gel phase incubated with 2-hydroxylated fatty acids. Statistics comparing the control with the 2OHFA treated sample: * p <0.05, ** <0.01 and *** <0.001.

FIGURE 6. Fluorescence spectroscopy analysis of membrane order and compactness in liposomes mimicking U-118 cell membrane composition (Table 1) incubated with polyunsaturated 2-hydroxylated fatty acids. **(A)** DPH steady state fluorescence anisotropy (3 nm bandwidth). **(B)** *t*-PnA mean fluorescence lifetime. Statistics comparing the control with the 2OHFA treated sample: * p <0.05, ** <0.01 and *** <0.001.

FIGURE 7. Membrane dipole potential measured through the excitation intensity ratio at 420 nm / 520 nm of di-4-ANEPPS in single phase liposomes (gel, l_d and l_o) with compositions given in Table 1 and effect of the indicated 2OHFA. Statistics comparing the control with the 2OHFA treated sample: * p <0.05, ** <0.01 and *** <0.001.

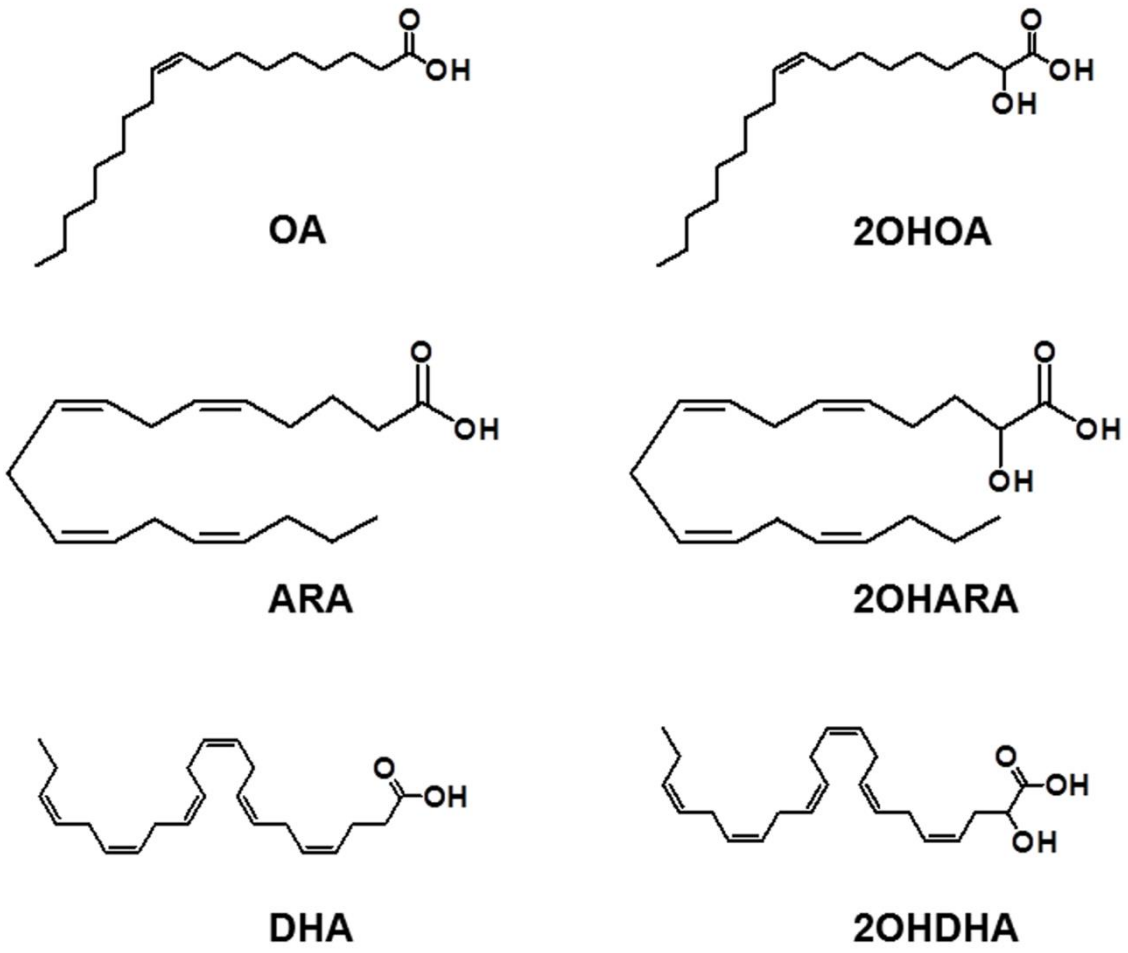

Figure 1

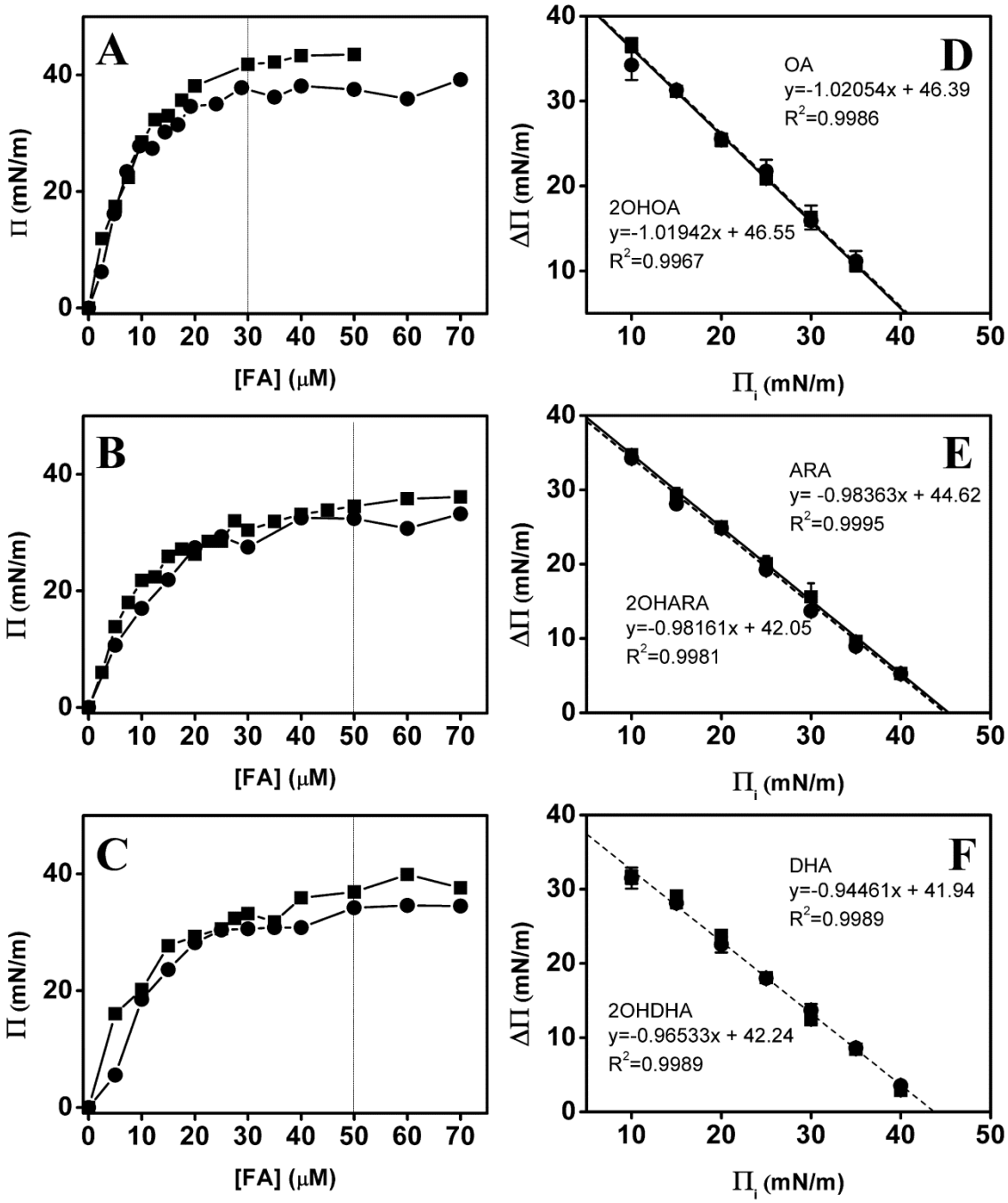
A
B
C
D
E
F
Π (mN/m)
[FA] (μM)
ΔΠ (mN/m)
Π_i (mN/m)
OA
y=-1.02054x + 46.39
R²=0.9986
2OHOA
y=-1.01942x + 46.55
R²=0.9967
ARA
y= -0.98363x + 44.62
R²=0.9995
2OHARA
y=-0.98161x + 42.05
R²=0.9981
DHA
y=-0.94461x + 41.94
R²=0.9989
2OHDHA
y=-0.96533x + 42.24
R²=0.9989

Figure 2

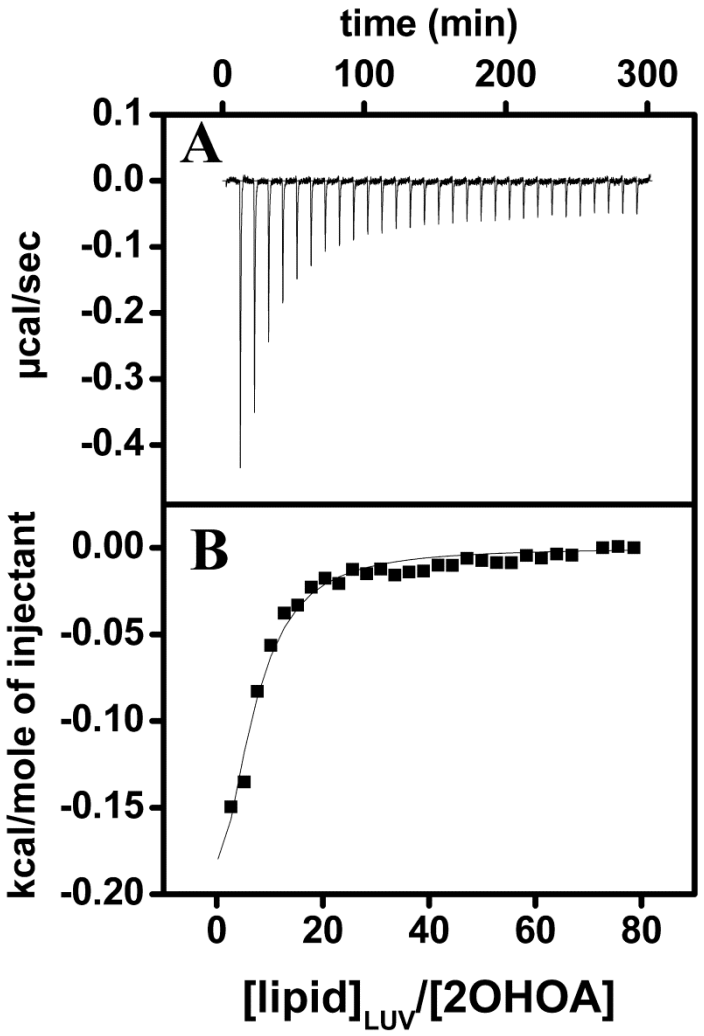
time (min)
0
100
200
300
A
0.1
0.0
-0.1
-0.2
-0.3
-0.4
µcal/sec
B
0.00
-0.05
-0.10
-0.15
-0.20
kcal/mole of injectant
0
20
40
60
80
[lipid]LUV/[2OHOA]

Figure 3

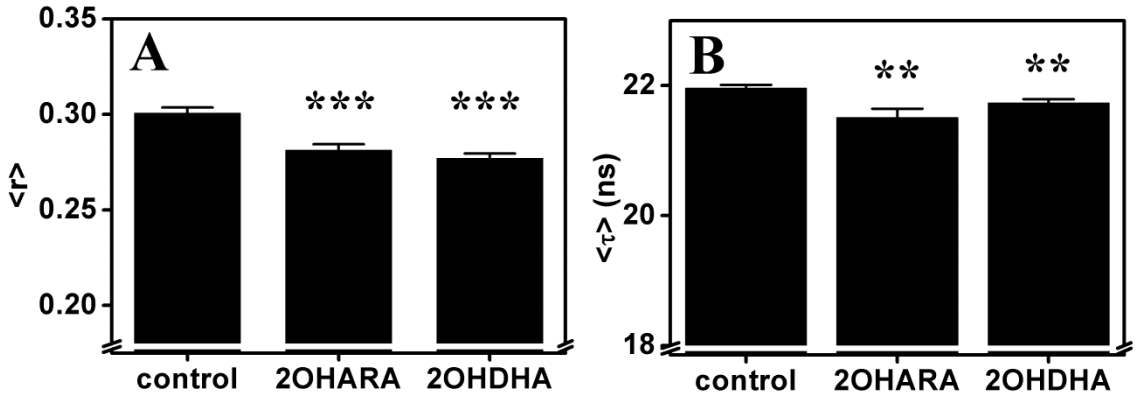
A
B
0.35
0.30
0.25
0.20
<r>
***
***
22
20
18
<τ> (ns)
**
**
control
2OHARA
2OHDHA
control
2OHARA
2OHDHA

Figure 4

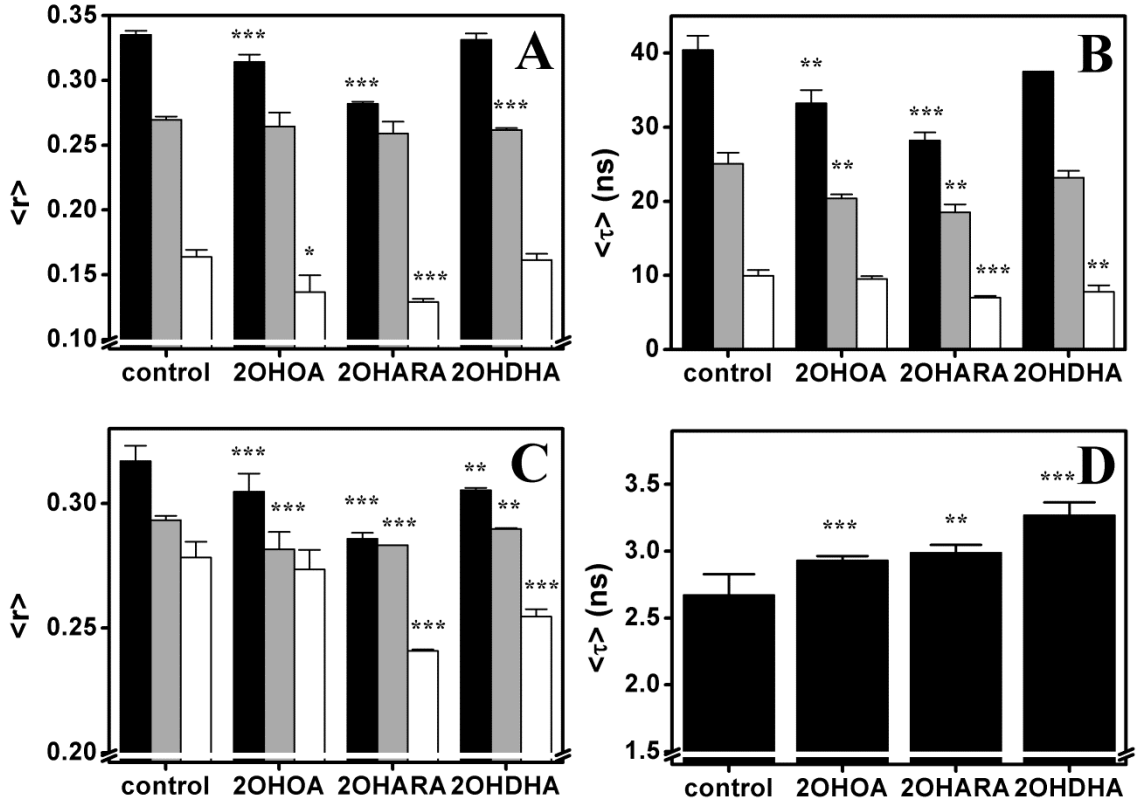

Figure 5

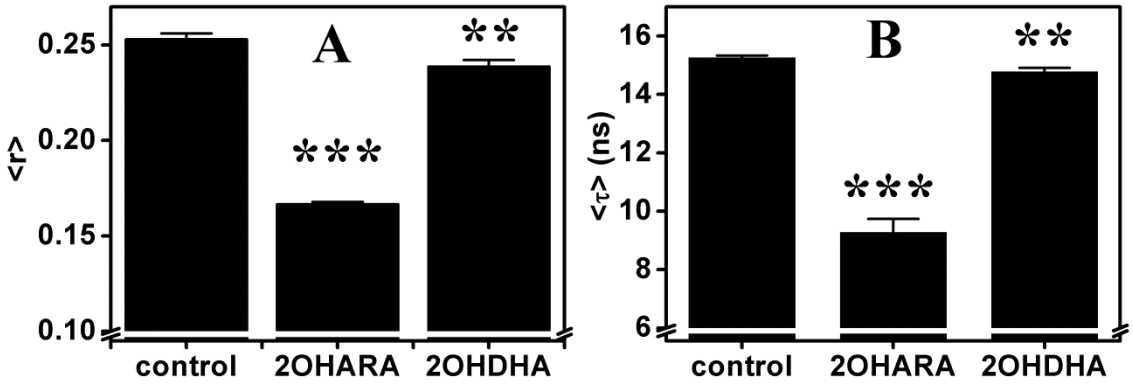

Figure 6

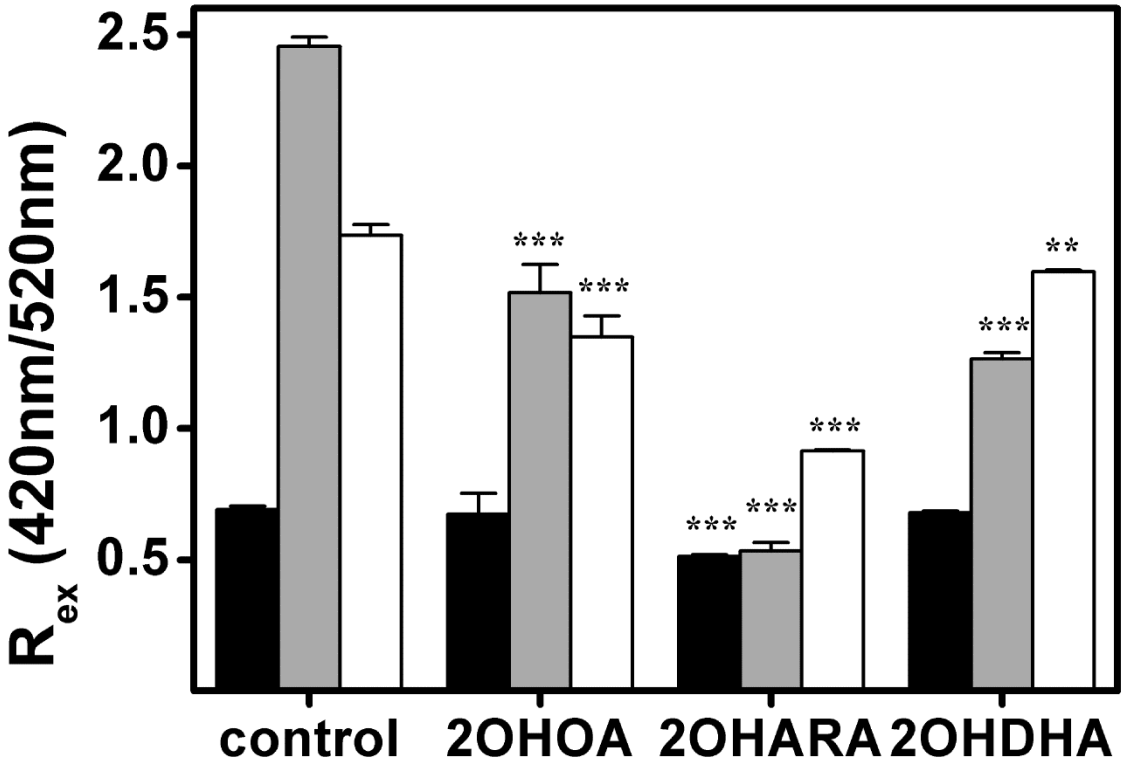

Figure 7

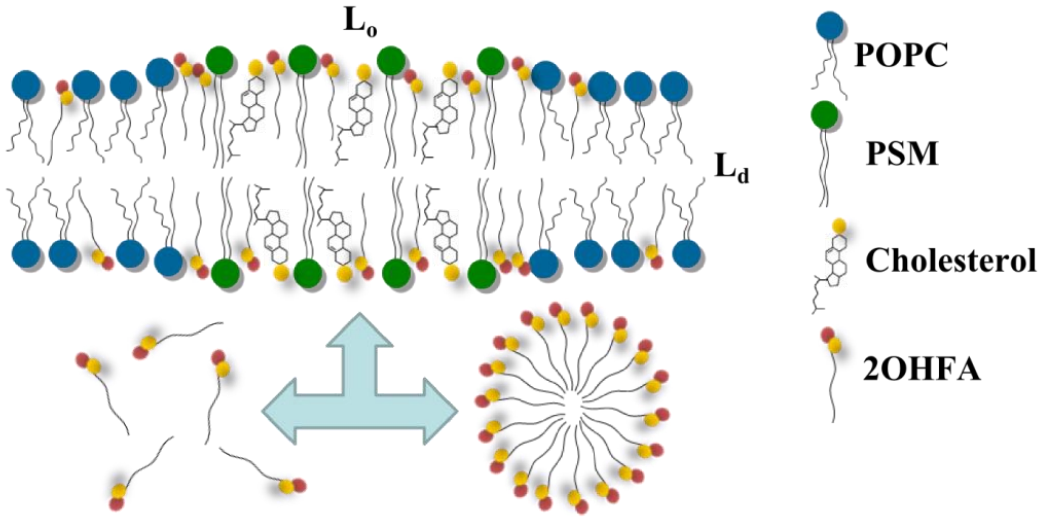

TOC graphic